ELSEVIER

Journal of Marine Systems 13 (1997) 225–244

JOURNAL OF MARINE SYSTEMS

Seasonal variability in sea surface oceanographic conditions in the Aegean Sea (Eastern Mediterranean): an overview

S.E. Poulos [a], P.G. Drakopoulos [b], M.B. Collins [c]

[a] *National Centre for Marine Research, Hellenikon 166 04, Athens, Greece*
[b] *Institute of Marine Biology of Crete, P.O. Box 2214, GR 71003, Iraklio, Crete, Greece*
[c] *Department of Oceanography, University of Southampton, European Way, Southampton SO14 3ZH, UK*

Received 15 May 1996; accepted 19 September 1996

Abstract

Seasonal variability and the spatial distribution of sea surface temperatures (SST) and salinities (SSS) are reviewed, in relation to the prevailing climatological conditions, heat fluxes, water budget and general water circulation patterns. Within this context, consideration is given to: sea surface temperatures; air temperatures; precipitation; evaporation; wind speeds and directions; freshwater (mainly riverine) discharges throughout the Aegean; and the exchange of water masses with the Black Sea and eastern Mediterranean Sea. The investigation of satellite images, covering a 6-yr period (1988–1994), has enabled a synthesis of the monthly sea surface thermal distribution to be established.

The climate of the Aegean Sea is characterised by annual air temperatures of 16–19.5°C, precipitation of about 500 mm yr^{-1} and evaporation of some 4 mm d^{-1}. The Aegean has a negative heat budget (approximately -25 W m^{-2}) and positive water balance ($+1.0$ m yr^{-1}), when inflow from the Black Sea is considered. During the summer, the (northerly) Etesians are the dominant winds over the Sea.

Mean monthly sea surface temperatures (SST) vary from 8°C in the north during winter, up to 26°C in the south during summer. SST depends mainly upon air temperature; there is a month's delay between the former and latter maxima. The sea surface salinity (SSS) varies also spatially and seasonally, ranging from less than 31 psu, in the north, to more than 39 psu, in the southeast; lower values (< 25 psu) occur adjacent to the river mouths. SSSs present their maximum differences during summer, whilst during winter and autumn the distribution of SSS is more uniform. The overall spatial SST and SSS distribution pattern is controlled by: distribution of the (colder) Black Sea Waters; advection of the (warmer) Levantine Waters, from the southeastern part of the Aegean; upwelling and downwelling; and, to a lesser extent, but locally important, freshwater riverine inflows.

Keywords: Aegean Sea; sea-surface temperature/salinity; ocean circulation; air–sea interaction; water balance

1. Introduction

The Aegean Sea constitutes the northeasterly part of the eastern Mediterranean Sea; it is bounded to the east by the Turkish coastline, to the north and west by the Greek mainland and to the south by the island of Crete (Fig. 1). The Aegean Sea is connected with the Sea of Marmara through the Dardanelles Strait and, hence, to the Black Sea through the Bosporus Strait. The Aegean Sea is connected with the Mediterranean Sea to the south, through the passages between Crete–Carpathos–Rhodos–Turkey

PII S0924-7963(96)00113-3

(southeast) and Crete–Kithira–Peloponnesos (southwest).

Recent developments in the field of deep water formation in the eastern Mediterranean Sea have shown that a water mass (the Cretan Intermediate Water), being formed in the southern Aegean Sea, exits through the Cretan Straits and sinks in the deep layers of the adjacent southeastern Ionian and northwestern Levantine Seas (Theocharis et al., 1992). Furthermore, during the hydrographic survey in Jan/Feb 1995 (R/V *Meteor* cruise), the influx of the Aegean Sea water was found to have replaced about 20% of the deep and bottom waters of the eastern Mediterranean basin (Roether et al., 1996). It was believed previously that the only source of such waters was the Adriatic Sea. The same authors have stated that this influx of Aegean waters, which has induced changes in the overall water characteristics and upward displacement of older waters of the Eastern Mediterranean, may have been caused by an increasing salinity of the Aegean Sea waters and possible alterations of the circulation pattern and its large-scale freshwater balance. Therefore, an updated review of the existing and accumulated (over the years) knowledge of the seasonal variability in the sea surface oceanographic conditions of the Aegean Sea will contribute to a better understanding of the operating processes.

The present investigation examines climatological factors and oceanographic processes which control changes in the sea surface temperature (SST) and salinity (SSS) of the Aegean Sea. Heat budget calculations, freshwater inputs and horizontal advection of sea water masses (i.e. Black Sea water inflow) are related here, to provide an estimate for the water balance of the Aegean Sea. Likewise, surface water circulation patterns are reviewed whilst, through the intercomparison of a series of satellite images, the seasonal variability and the spatial distribution of SST are revealed.

The study is based upon published information, data sets (e.g. COADS, MED-4 gridded seasonal fields) and raw data provided by the Hellenic Meteorological Service and the Hellenic Hydrographic Service. Finally, sectorised enlargements of AVHRR (Advanced Very High Resolution Radiometer) greytone thermal images from NOAA-9 and NOAA-11 satellites were provided by the NERC Receiving Station (University of Dundee). Detailed descriptions regarding the published information, data sets and raw data are presented in the relevant sections, as described below.

2. Geomorphological setting

The Aegean Sea covers an area of approximately 1.8×10^{11} m^2 and contains a water volume of some 7.4×10^{13} m^3 (Hopkins, 1978). The basin has a complex topographical structure, with irregular bathymetry, a multifarious coastline and hundreds of small and large islands (Fig. 1). The bottom topography consists of three main depressions: (i) the North Aegean Trough, which accommodates the Sporades Basin (1500 m maximum depth) and the Mount Athos Basin (1000 m maximum depth); (ii) the Chios Basin within the central part, with depths of up to 1100 m; and (iii) the Cretan Basin. The latter feature is the largest and the deepest depression within the region, with water depths exceeding 2000 m (to the north of the eastern end of the island of Crete). The shallower parts of the Sea (< 200 m) consist of the Thermaikos, Samothraki, and Cyclades Plateaus (for locations, see Fig. 1).

At its northeastern extremity, the Aegean Sea exchanges flows with the Sea of Marmara: this acts as a conduit between the Aegean and Black Seas. The Sea of Marmara is an almost completely enclosed depression, with a surface area of 11,500 km^2 and an overall volume of 3378 km^3; it is connected to the Black Sea through the Bosporus Strait (trending NNE–SSW) and with the Aegean Sea through the Dardanelles Strait (trending NE–SW). The Bosporus is about 31 km long and 0.7–3.5 km wide, with an average depth of 35 m. The Dardanelles Straits are longer (nearly 62 km), wider (1.3–7 km) and deeper (average depth 55 m) (Ergin et al., 1991).

To the south, the Aegean Sea communicates with the eastern Mediterranean Sea through the Cretan Straits. Communication at its southeastern limit takes place through the passages between the islands Crete and Casos (depth 700 m, width 67 km), Carpathos and Rhodos (depth 550 m, width 43 km) and Rhodos and Turkey (depth 350 m, width 17 km). The southwestern strait consists of the following passages: Crete–Antikithira (depth 700 m, width 32 km); An-

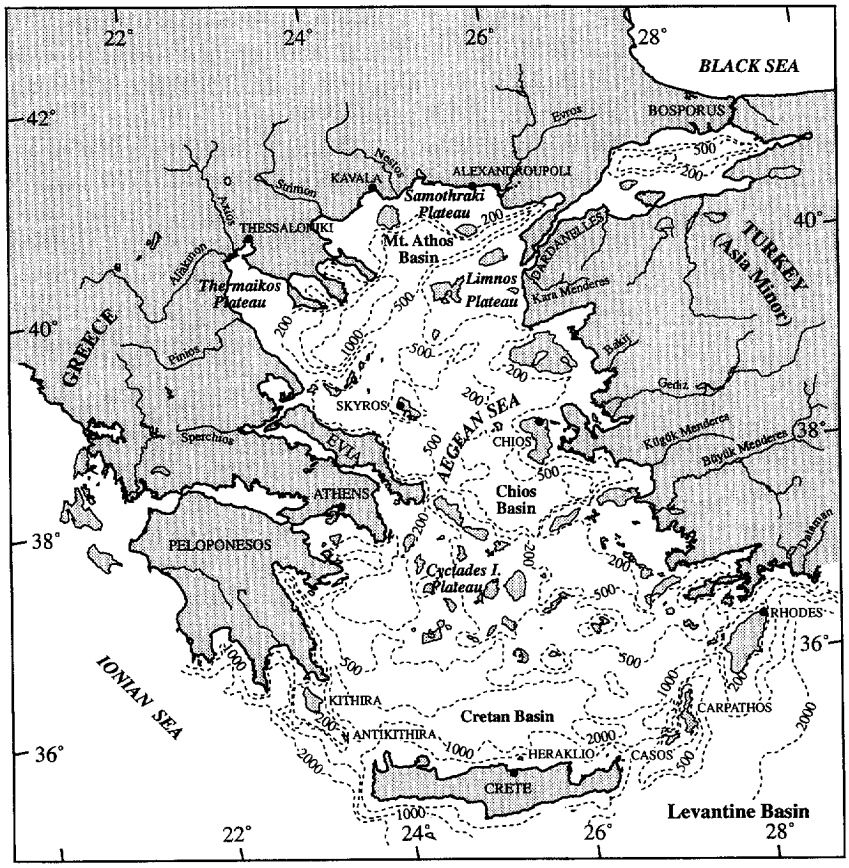

Fig. 1. The Aegean Sea: bathymetry (in metres) and locations of the main hydrographic basins and plateaus.

tikithira–Kithira (depth 60 m, width 33 km); and Kithira–Peloponnesos (depth 180 m, width 11 km) (Hopkins, 1978).

3. Climate

The Aegean Sea is characterised by a typical Mediterranean-type of climate. The annual climatic variability can be divided into two main periods: (i) November to March, which is cool and rainy; and (ii) May to September, which is a hot and rather dry season. October and April can be characterised as intermediate months, between these two distinctive periods (Zabakas, 1981).

3.1. Air temperature

The mean annual air temperature over the Aegean Sea varies between 16°C and 19.5°C, increasing towards the south. The absolute minimum and maximum air temperatures over parts of the surrounding mainland occasionally reach −25°C (winter) and +45°C (summer), respectively (Zabakas, 1981). For the period 1975–1990, data obtained from the Meteorological Service showed that the lower mean monthly winter values varied from 4.8°C (Alexandroupolis) to 12°C (Heraklio). During summer, the mean monthly temperatures lie between 24°C (Kavala) and 26.5°C (Rhodos). The former mean monthly air temperatures represent daily average values of dry and wet bulb thermometer readings, respectively.

3.2. Precipitation

Annual precipitation over the Aegean Sea varies generally between 400 and 700 mm per annum

(Tixeront, 1970), with a mean annual relative humidity of between 65% and 75%. In general, the rainfall is limited (or does not occur) throughout the summer months; likewise, it is more pronounced over the eastern part of the Aegean. Observed levels of precipitation, representing mean monthly precipitation levels based upon daily average measurements over a 16-year period (1975–1990), were between 372 mm (Athens) and 672 mm (Rhodos), with an overall mean value of some 495 mm yr^{-1}.

3.3. Wind

The wind field of the Aegean Sea is dominated by winds blowing from the north. South-southwesterly winds occur during spring, whilst diurnal sea-breezes occur along the Greek and Turkish coasts during summer. Mean monthly wind speeds, for the period 1980–1983 vary between about 3 m s^{-1} (Chios in December, or Rhodos in January) to > 7.5 m s^{-1} (Chios in February and August) (Jakovides et al., 1989). The seasonal wind stress distribution over the Aegean Sea is presented schematically in Fig. 2 (May, 1982).

The annual variation in the wind regime is related mostly to the persistence of the northerly winds,

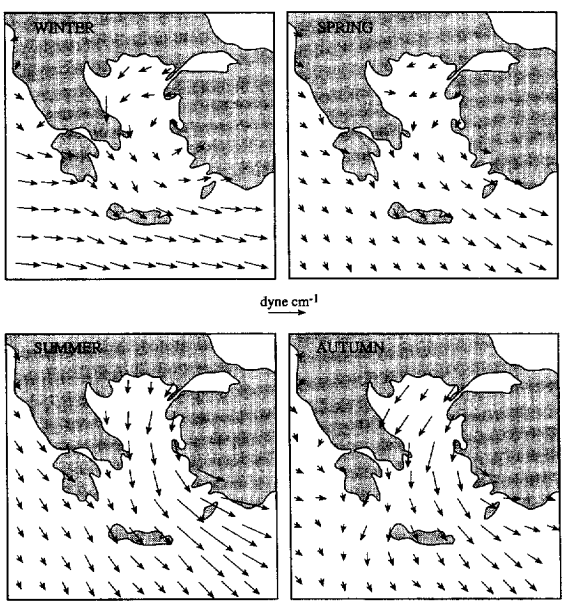

Fig. 2. Seasonal variation in wind stress over the Aegean Sea (after May, 1982).

which present a double fluctuation: a primary maximum during winter (December–February), together with a secondary maximum during summer (July–August).

During winter, strong, cold and dry northerlies (generated by the outbreak either of the Arctic or the Polar continental air masses) are funneled through the valleys of the rivers Axios (the Vardar zone), Strimon and Evros, towards the Aegean Sea (Theocharis and Georgopoulos, 1993). In addition, the Aegean Sea occasionally experiences southerly winds (Catsoulis, 1970).

During the warm period (May–September), the wind field of the Aegean is dominated by the presence of the Etesian wind; this is a northerly wind system, associated with clear skies, which persists for extended periods and often reaches gale force in strength. Dynamic parameters involved in the generation of the winds are: (i) the high pressure system of the Azores which, in summer, moves north and extends to southeastern Europe and the Balkans; (ii) the deep Asiatic Low which extends west, sometimes farther than Cyprus; (iii) the western Russia high pressure system; and (iv) the high pressure fields of northwestern Europe, which often reach the Aegean (Lascaratos, 1992). Elsewhere, the Etesians have been classified (Carapiperis, 1968) in terms of their mean daily velocity, into weak (≤ 3.3 m s^{-1}), moderate (3.4–7.9 m s^{-1}) and strong (≥ 8 m s^{-1}).

The maximum wind force axis extends from the northern Aegean, passes slightly to the east of Lemnos and Skyros, through the Cyclades, past the island of Carpathos and on toward the centre of the eastern Levantine Sea (Fig. 1). Early investigations have identified that, in the Cyclades islands, there is a $> 20\%$ frequency of wind speeds ≥ 6 Beaufort and $> 10\%$ of ≥ 7 Beaufort, during summer (Metaxas, 1973).

3.4. Evaporation

Jakovides et al. (1989), analysing four years (1980–1983) of continuous daily-averaged meteorological data from 4 stations in the Aegean (i.e. Lemnos, Chios, Skyros and Rhodos), have found that mean annual evaporation over the Aegean Sea is 4.2 mm d^{-1} (using the Businger et al. (1971) bulk aerodynamic formula). The former value is very

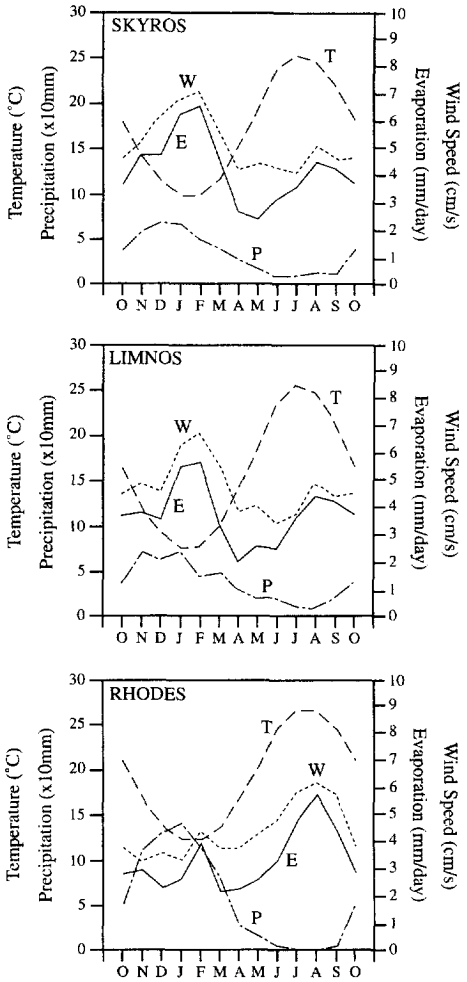

Fig. 3. Monthly variations in air temperature (°C), precipitation (mm), wind speed (m s^{-1}) and evaporation (mm d^{-1}) (for station locations, see Fig. 1).

close to that of 3.9 mm d^{-1} obtained by Bunker et al. (1982) for larger parts of the Mediterranean, using the formula of Businger et al. (1971). For comparison, lower annual evaporation (3.6 mm d^{-1}) has been calculated during the present investigation (Section 4), on the basis of a monthly observations averaged for a longer period (1945–1990; COADS data set) than used previously.

Evaporation fluctuations follow those of air temperature, precipitation and wind speed, as shown on Fig. 3; it is at a minimum (2 mm d^{-1}) in late spring and autumn, and a maximum (5–7 mm d^{-1}) in February and July/August (Jakovides et al., op cit.). Minimum evaporation values in spring may be the result of reduced wind speeds and due to the fact that sea surface temperatures are not as high as they become three months later. In autumn, the minimum evaporation can be attributed to a reduction in the Etesian winds (see below) and the fact that depressions rarely pass over the Aegean Sea, at this time.

4. Heat fluxes

The net heat flux through the sea surface into the ocean waters is made up generally of the incoming solar radiation (Q_s), minus the back longwave radiation (Q_b) and the turbulent fluxes of latent heat (Q_e) and sensible heat (Q_h). The several empirical formulae and coefficients used often to calculate the components of the heat flux balance are still under development and the available data needed to evaluate them are not adequate; this results in considerable uncertainty in the estimation of an oceanic heat budget. However, various authors (Bunker, 1971; Bunker et al., 1982; May, 1983; Jakovides et al., 1989 and Bethoux and Gentili, 1994) have attempted to estimate components of the heat flux budget in the Aegean Sea, usually as part of the overall Mediterranean Sea budget.

For the needs of the present study, the long-term average and seasonal heat fluxes for the Aegean Sea have been calculated following an approach similar to that of Garrett et al. (1993) and Gilman and Garrett (1994). The source of data was the COADS (Comprehensive Ocean Atmospheric Data Set, based mainly upon observations undertaken by ships of opportunity e.g. Woodruff et al., 1987) database for the period 1946–1990. Observed parameters required for this analysis were: SST, air temperature, air pressure, saturation humidity, specific humidity, wind speed and cloudiness. The estimation of the incoming solar radiation was based upon the formula of Reed (1977). For the net longwave back-radiation, the recent bulk formula of Bignami et al. (1991) has been utilised. For the evaporation and sensible heat coefficients, the tables of Smith (1988) have been incorporated. It should be noted that the surface heat flux of the whole Mediterranean basin was calculated initially, then the solar radiation was scaled

Table 1
Long-term heat flux components derived for the Aegean Sea, as estimated by different authors

	Q_s (W m^{-2})	Q_b (W m^{-2})	Q_e (W m^{-2})	Q_h (W m^{-2})	Q_t (W m^{-2})
Bunker (1971)			−147		
May (1983)	192	−69	−131	−18	−26
Jakovides et al. (1989)			−130		
Bethoux and Gentili (1994)			−147		−38
The present study	169	−78	−104	−13	−26

Note: Q_s, solar radiation; Q_b, back radiation; Q_e, latent heat; Q_h, sensible heat and Q_t, net heat flux.

properly in order for the heat flux to balance the relatively well-known net heat flux through the Strait of Gibraltar (~ -7 W m^{-2}, cf. Garrett et al., 1993). Furthermore, wind speeds were re-scaled to compensate for the underestimation introduced by the algorithm used to convert Beaufort scale to wind speed (Kaufeld, 1981).

The results of the present analysis, together with those of the previously quoted studies, are presented in Table 1. Differences between the results reflect the diversity in the formulae and the data sets used. Nevertheless, there is agreement between the derived results that the average annual net heat flux within the Aegean is negative (here, -26 W m^{-2}). This observation implies that the Aegean Sea is, on average, loosing heat through its surface. The balance is maintained by the advection of warm Levantine waters, through the Cretan Straits. It has been estimated that the heat exchange with the Black Sea is equivalent to a surface flux of no more than 1 W m^{-2} (Tolmazin, 1985). This heat budget deficit, the combination of surface heat loss and the resulting advection, drives the thermohaline circulation in the Aegean Sea.

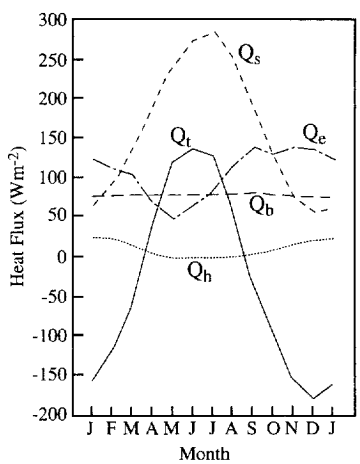

Fig. 4. Monthly variation in the heat flux components of the Aegean Sea: Q_t, net heat flux through the sea surface; Q_s, incoming solar radiation; Q_b, longwave radiation; Q_e, latent heat flux and Q_h, sensible heat flux (Note: the components Q_e, Q_h and Q_b are inverted i.e. a maximum value corresponds to a maximum loss).

In terms of the seasonal cycle, the net heat flux was found to reach a maximum positive value during June; this coincides with the insolation maximum. Meanwhile, the latent heat flux reaches a maximum during autumn and early winter (Fig. 4). This pattern is in response to the strong and cool winds present over the Aegean Sea during this period. The loss due to sensible heat is at a maximum during winter, whilst the longwave radiation has negligible seasonal variability.

The annual spatial distribution of the heat flux components (Q_t, Q_e, Q_h and Q_b) are depicted in Fig. 5. There is a N–S gradient, with maximum heat loss taking place in the northern Aegean (> -35 W m^{-2}) and a minimum value in the Cretan Sea (~ -10 W m^{-2}). The latent heat evaporation maximum (> 115 W m^{-2}) occurs in an area between the Cyclades Plateau and the Asia Minor coast. Generally, the overall values decrease towards the west. The sensible heat loss has a N–S gradient, increasing towards the north. The longwave back radiation is fairly uniform, varying between 77 and 79 W m^{-2}.

5. Water budget

5.1. Black Sea Waters

The Aegean Sea receives the colder and less saline Black Sea Water though the Sea of Marmara

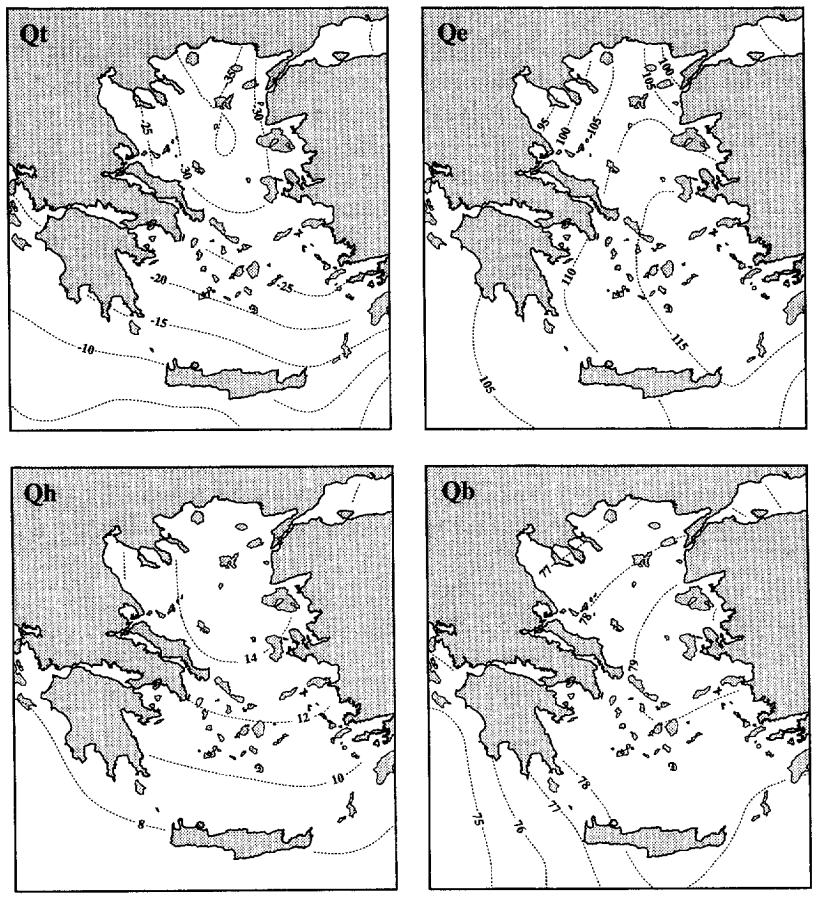

Fig. 5. Mean annual spatial distribution of the heat flux components: Q_t, net heat flux through the sea surface; Q_e, latent heat flux; Q_h, sensible heat flux; and Q_b, longwave radiation.

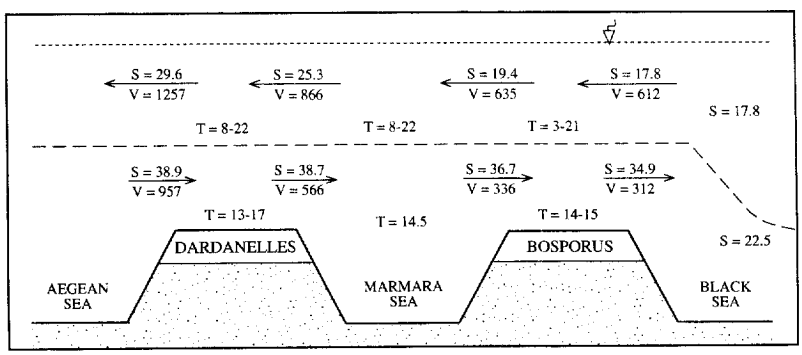

Fig. 6. Water exchange between the Aegean Sea, Sea of Marmara and Black Sea, through the Dardanelles and Bosporus Straits (from Unluata et al., 1990). Key: S salinity, in psu; T temperature, in °C; V volume, in $km^3\ yr^{-1}$.

and the associated Bosporus Strait (between Marmara and the Black Sea) and the Dardanelles Strait (between Marmara and the Aegean Sea) (see Fig. 1). Within the Straits and the Sea of Marmara, two-layer stratification and opposing flow circulation has been established, on the basis of density differences between the Aegean and Black Sea Waters (Oguz and Sur, 1989 and Yuce, 1996).

The two different water masses are separated by a pycnocline, at an average depth of 25 m. The density profile is dominated by salinity, even though there are significant seasonal variations in water temperature. The upper layer is occupied by the less saline Black Sea Waters (BSW) and the lower layer by the denser Aegean Sea Waters (ASW) (Unluata et al., 1990). The surface layer in the Dardanelles flows towards the Aegean Sea, at velocities of 50–200 cm s^{-1} (with an average of 80–90 cm s^{-1}). The bottom layer moves in the opposite direction, towards the Sea of Marmara, with velocities ranging from 20–40 cm s^{-1} (Ergin et al., 1991). Mean annual temperature (T, °C), salinity (S, psu) and water fluxes (Q, km^3 yr^{-1}) are presented schematically in Fig. 6, for the Sea of Marmara and the Bosporus and Dardanelles Straits. Some 1257 km^3 of colder and fresher water flows annually into the Aegean Sea whilst, at the same time, 957 km^3 of the more saline Aegean Sea Water enters the Sea of Marmara through the Dardanelles Strait (Unluata et al., 1990).

Inevitably, the surface water outflow and bottom water inflow fluxes vary seasonally, as they are dependent upon wind stress and density differences above and below the pycnocline. Thus, the largest flow towards the Aegean occurs in late spring and summer, corresponding to periods at which the precipitation and river runoff discharged into the Black Sea increases substantially (Oguz and Sur, 1989). In general, the net annual flow ($BSW_{surface} - ASW_{bottom}$) through the Dardanelles Strait is some 300 km^3 yr^{-1}.

5.2. River inputs

The Aegean Sea receives the freshwater outflows from various rivers discharging along the Greek and

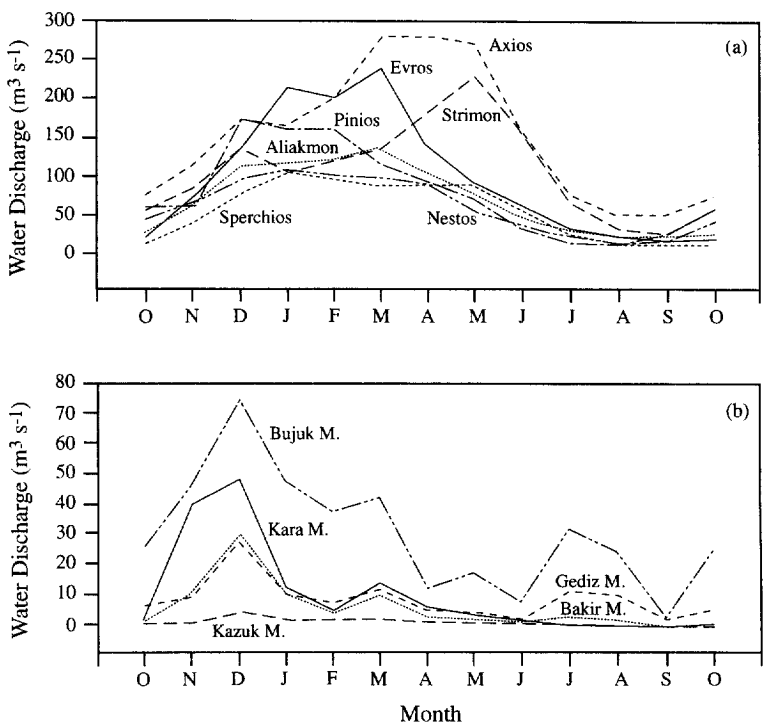

Fig. 7. Mean monthly variation in freshwater inputs (m^3 s^{-1}) from rivers discharging along the Greek (a) and Turkish (b) Aegean Sea coastlines (for locations, see Fig. 1).

Turkish coastlines (Fig. 1). The main inputs are: the rivers Axios, Aliakmon, Gallikos, Pinios which discharge into Thermaikos Gulf (northwestern Aegean Sea); the R. Sperchios, along the western coastline; the rivers Evros, Strimon and Nestos along the northern Greek shoreline and the smaller rivers (K. Menderes, Bakir, Gediz, Kuguk Menderes and Bujuk Menderes) discharging along the eastern (Turkish) coastline. The mean annual freshwater discharge and total runoff of these rivers are listed in Table 2.

In addition to the riverine supply, a substantial "freshwater" input is contributed by the sewage outfall of the numerous cities located adjacent to the coastlines; for example, Athens discharges some 219 $\times 10^6$ m^3 yr^{-1} of waste (Theodorou, 1992). Interestingly, this latter figure is comparable to the total water annual discharge of the smaller Turkish rivers.

The rivers discharging into the Aegean Sea show different monthly variations in water inputs (Fig. 7). In general, rivers discharging along the Greek coastline are associated with high water discharge levels between December and April. Turkish river discharges are at a maximum from October to March

Table 2
Mean monthly and annual river discharges into the Aegean Sea

	Drainage area (km^2)	Mean annual discharge (m^3 s^{-1})	Mean annual runoff (m^3 10^6)
Greece [a]			
Ebros	27,465	103	3250
Nestos	4374	58	1819
Strimon	10,937	110	3440
Axios	22,450	159	5031
Aliakmon	6075	73	2292
Pinios	7081	81	2529
Sperchios	1158	62	743
Turkey [b]			
Karamenderes	1586	11.1	345
Bakircay	16,463	6.5	204
Gediz Nehri	15,617	9.0	283
Kuzukmenderes	3255	1.1	33
Bujuk Menderes	19,596	30.9	370

Note:
(a) Greek river water discharge data, covering the period 1962–1972, abstracted from Therianos (1974).
(b) Turkish river water discharge data, covering the period 1978–1982, abstracted from E.I.E. Water Year Discharges [*E.I.E. Publications Series* (1981–1985), Ankara (in Turkish)].

Table 3
The main components of the annual water balance of the Aegean Sea

	Present study [a] (mm yr^{-1})	Published information (mm yr^{-1})
Precipitation (P)	500	
Evaporation (E)	1280	1830 [c]
River runoff (R)	110	
Black Sea Water (BSW)	1670 [b]	
Water balance (Wb) [d]	1000	1450 [e]

Note:
[(a)] the area of the Aegean Sea has been taken as being equal to 1.8×10^{11} m^2 (after Hopkins, 1978).
[(b)] after Ergin et al. (1991).
[(c)] after Bethoux and Gentili (1994).
[(d)] $Wb = P + R + BSW - E$.
[(e)] value is based upon the $(E) = 1830$ mm yr^{-1}.

responding directly to rainfall levels over their catchments, whilst the Greek catchments incorporate water fluxes attributed also to freshwater springs and snowmelt.

The total amount of freshwater water inputs to the Aegean Sea is around 2×10^{10} m^3 yr^{-1}, when the inputs of the numerous small ephemeral rivers and torrents are incorporated into the total water discharge of the main river systems presented in Table 2.

5.3. Water balance

The annual amount of evaporation (E) over the region exceeds the sum of precipitation (P) and river runoff (R). However, if the net Black Sea Water inflow (BSW) is considered, then the water balance of the Aegean Sea is positive (i.e. $P + R + BSW - E > 0$). The excess of water mass, per unit area, in the Aegean has been calculated to be between 1 and 1.4 m yr^{-1} (Table 3). For comparison, Bethoux and Gentili (1994), established the water budget of the whole of the Mediterranean Sea and have estimated a positive water balance for the Aegean of the order of 0.7 m yr^{-1}. These calculations have not taken into account water advected towards and away from the Aegean, through the Cretan Straits. Such exchanges are a few orders of magnitude greater than those attributed to evaporation, precipitation, river runoff and Black Sea water fluxes. For example, Bethoux

(1980) has estimated that some 15.2×10^{12} m^3 yr^{-1} enter the Aegean Sea from the straits between Rhodos and Crete, and about 9.84×10^{12} m^3 yr^{-1} leave the Aegean Sea between the island of Crete and the Greek mainland (Peloponnesos). These calculations of mean annual fluxes of surface waters have been based upon the spatial variations in salinity, combined with an existing knowledge of water circulation. Further, it is believed that the exchange of water masses through the Cretan Straits is not constrained by inward flow at the surface and outward flow at the bottom, but is imposed by the general water circulation patterns (Hopkins, 1978). Finally, recent numerical modelling studies of the general circulation of the Mediterranean basin have shown a net inflow from the eastern Cretan straits balanced by a net outflow from the western straits and equal to 5×10^{13} m^3 yr^{-1} (P.G. Drakopoulos and A. Lascaratos, pers. commun.).

6. Circulation of surface waters

The surface water circulation pattern of the Aegean Sea is not simple and regular, but changes temporally and seasonally. For example, sporadic and strong meteorological events (i.e. gale force winds) can alter local water circulation patterns. The complex circulation is due to many factors, such as: the geographical distribution of the various Aegean island chains; the irregular bottom topography throughout the region; inflow of the lower temperature and salinity Black Sea Waters; the river outflows from the Greek and Turkish mainland; seasonal changes in the meteorological conditions (with the most pronounced example being the summer presence of the Etesian winds, with associated upwelling and downwelling).

The general surface water circulation pattern of the northern and southern parts of the Aegean Sea are presented in Fig. 8.

The winter circulation pattern, described initially by Ovchinnikov (1966), consists of a cyclonic gyre within the northern basin of the Aegean Sea (Fig. 8a); this is associated with the northerly movement of sea water along the southern part of the eastern coast of Turkey, together with southerly movement along the eastern coastline of Greece. The presence

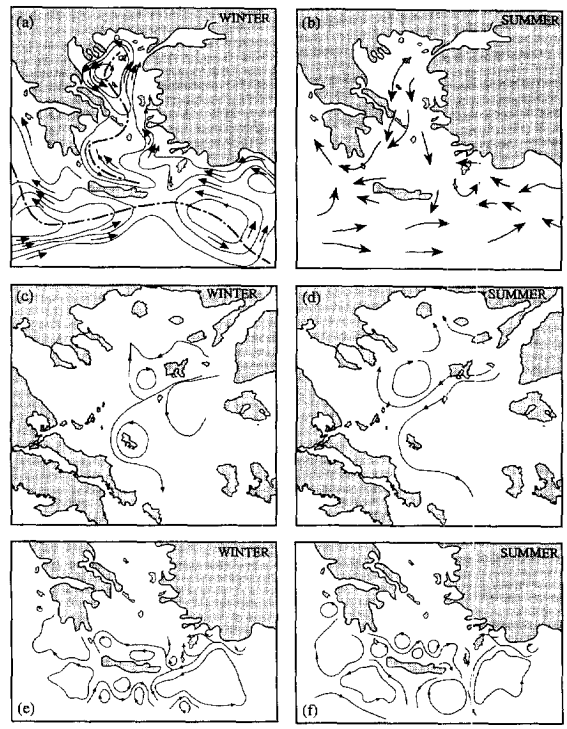

Fig. 8. Principal circulation patterns of the surface waters of the Aegean Sea, in winter and summer: (a) Ovchinnikov (1966); (b) Lacombe and Tchernia (1972); (c) and (d) Zodiatis (1994); (e) and (f) Theocharis et al. (1993). Note: vectors indicate flow direction, whilst the dashed line indicates a convergence zone. In (c) and (d) the vectors represent schematically-generalised flow patterns, derived from numerical model graphical outputs.

of the gyre in the northern Aegean Sea has been identified also by Roufogalis (1971a,b), Theocharis and Georgopoulos (1993) and Zodiatis (1994), on the basis of water temperature and salinity distribution patterns.

The most pronounced characteristic of the circulation in the North Aegean is the spreading of the BSW inflow from the Dardanelles. Zodiatis (1994), investigating the advection of BSW in the northern Aegean Sea, found that it is related to the general westward, then southward, water movement associated with small-scale cyclonic and anticyclonic flow regions (Fig. 8c). The waters flow westward along the northern shoreline of Limnos, where they bifurcate into northerly and southerly directions. In addition, the spreading of the BSW is characterised by an interannual variability; this results from changes in

the dynamic regime of the area (e.g. wind stress) (Zodiatis, 1994). Another interesting feature is the formation of the frontal zone, over the Limnos Plateau, between the colder and less saline BSW and the saltier and warmer Levantine Waters (LW); these propagate along the eastern Aegean Sea, intruding occasionally up to the Samothraki Plateau. At this latter location, a dense and oxygen-rich water mass is formed; this sinks subsequently, contributing to the ventilation of the deep waters of the northern Aegean Sea (Theocharis and Georgopoulos, 1993).

The winter circulation pattern (Fig. 8e) within the southern part of the Aegean (between the Cyclades islands and Crete) consists of two smaller cyclonic gyres, together with a general inflow of water from the Levantine Basin through the strait of Crete–Carpathos–Rhodos–Turkey. There is outflow through the Crete–Kithira passages and a general westerly movement of the waters to the north of Crete (Theocharis et al., 1993; Zodiatis, 1993).

The summer surface water circulation of the Aegean Sea (Fig. 8b) is characterised by general southerly movement (Lacombe and Tchernia, 1972). Such motion, which succeeds the winter cyclonic circulation, is induced by the prevailing wind climate; this, in turn, is dominated by the Etesians (Metaxas, 1973). Further, diurnal sea breeze systems prevail along both the Greek and Turkish coastlines.

The Etesians generate a coastal divergence and surface water flow towards the south, along the eastern boundary of the Aegean, which causes coastal upwelling. This latter phenomenon relates to a decrease in the sea surface temperature, by about 2°C, which enhances the adiabatic air cooling; it contributes, therefore, to the stability of the wind system (Hopkins, 1978). On the western boundary of the Aegean, however, these winds induce a coastal convergence compatible with a southerly surface flow associated with coastal downwelling. Under such conditions, the unique (single) winter cyclonic gyre is succeeded by a 2-gyre system incorporating an anticyclonic part to the east and a cyclonic part to the west; these are separated by a divergence zone, where upwelling phenomena may occur. Such a pattern has been presented also by Zodiatis (1994), for the summer period in the North Aegean Sea (Fig. 8d). Furthermore, the same author has stated that BSW during the warm periods (summer–autumn) flow, in general, in a southwesterly direction. The core of this water mass is located to the south of Limnos island.

In summer the water circulation in the southern Aegean Sea appears to have been modified by a local gyre system (Fig. 8f), with general easterly movement along the northern coastline of Crete. In addition, the inflow during winter at the southeastern limit of the Aegean Sea is now restricted to between Rhodos and Turkey. At the Rhodos–Carpathos and Carpathos–Crete passages, such a flow has been replaced by an outflow towards the Levantine Basin (Theocharis et al., 1993).

Finally, the application of the Princeton Ocean Model (POM), designed originally by Blumberg and Mellor (1987), has revealed that the principal driving mechanism of the surface circulation pattern is the wind stress in combination with the advection of water fluxes (e.g. Black Sea Water, Levantine Water). Especially for the winter season, the model results show the presence of a multi-cyclonic system in the northern Aegean Sea, whilst a simple cyclonic pattern is present in the Cretan Sea (southern Aegean Sea) (Nittis et al., 1995). These results are in a good agreement with the winter circulation pattern proposed by Ovchinnikov (1966). For the summer period, model simulation of the surface water circulation is generally anticyclonic. Furthermore, in the northern Aegean Sea (Chios basin) a double-gyre system (cyclonic to the west and anticyclonic to the east) exists (Nittis et al., 1995); this is similar to that described by Hopkins (1978) and Zodiatis (1994).

7. Sea surface temperature and salinity

The seasonal Sea Surface Temperature (SST) and Salinity (SSS) observations used in the present study and referred to the open sea have been obtained from the MED-4 gridded seasonal fields (Brasseur et al., 1996). These fields are the result of objective analysis of the raw data contained in the MODB data-base.

The main factor affecting sea surface temperatures (SST) are the seasonal atmospheric conditions, which are reflected in the air temperature (AT). For example, Theoharatos and Tselepidaki (1990) have established that the cross correlation coefficient (r) between SST and AT, for 15 stations from the

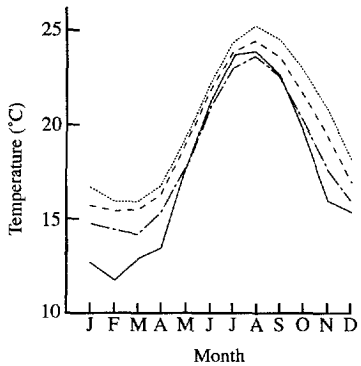

Fig. 9. Monthly variation in sea surface temperature (°C) from 4 selected areas of the Aegean Sea. These areas represent 2°×2° boxes of the COADS data, with their southwesterly limit being at the geographical coordinates (long., lat.): (A) (24°, 40°), (B) (24°, 38°), (C) (24°, 36°) and (D) (24°, 34°).

Aegean Sea, is $r^2 > 0.80$ (significant at the 95% level). Further, monthly variations in SST and AT show that, on an annual basis, the sea temperature appears to lag in relation to that of the overlying airmass, by the order of a month. Finally, principal component analysis carried out by Vlahakis and Pollatou (1993) has shown that SST changes, related to AT fluctuations, occur almost simultaneously throughout the Aegean Sea.

In Fig. 9, the monthly distribution of SST has been plotted for selected areas covering the whole of the Aegean Sea. Notably, the temperature of the BSW is lower than the SST of the northern Aegean Sea throughout the year. The annual maximum SST values (> 24°C) occur around August; minimum values (< 13°C) are reached in February, although

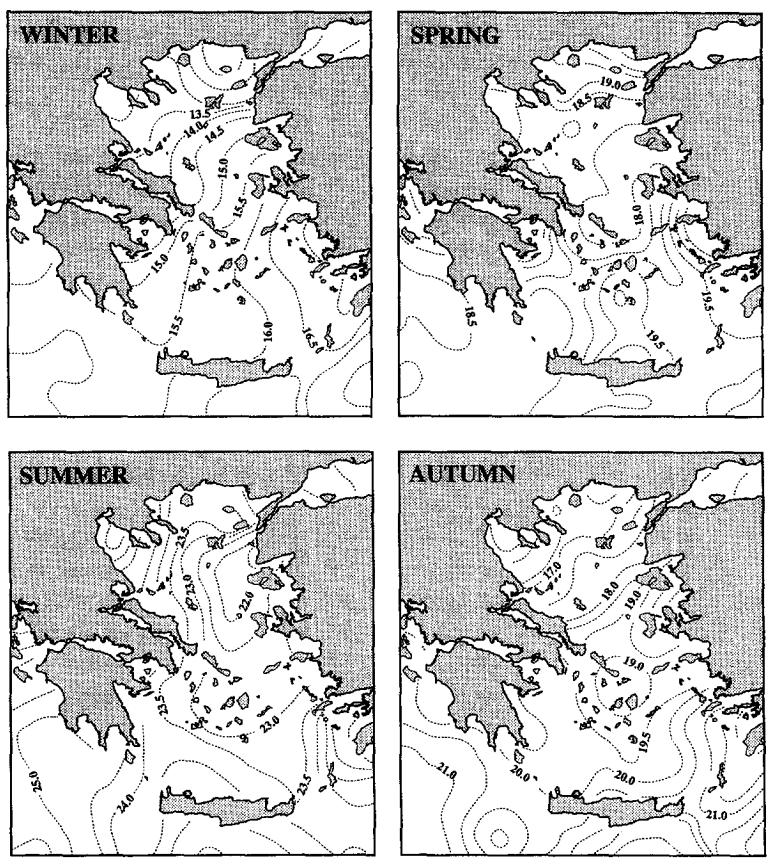

Fig. 10. Seasonal spatial distribution in sea surface temperature (in °C) over the Aegean Sea.

there are a few exceptions where the minimum occurs in January. Besides, the spatial and seasonal distribution pattern of the SST in the Aegean Sea is presented in Fig. 10. A similar distribution pattern of SST in winter and summer, for the northern Aegean Sea (to the north of Cyclades Plateau) has been also described by Zodiatis and Balopoulos (1993).

Sea Surface Salinity (SSS) values vary seasonally, ranging from less than 31.0 psu to more than 39.0 psu. Further, lower values (< 25 psu) have been measured nearby the river mouth areas. The salinity distribution (Fig. 11) presents generally a N–S trend with the less saline waters present towards the north. The relatively lower salinity values, presented for the north and within the coastal embayments, are associated with the BSW inflow and the freshwater riverine inputs. The former situation is more pronounced during spring and early summer, when the river discharges reach their maximum values (Fig. 7). The more saline surface waters cover the southeastern part of the Aegean, flowing in from the adjacent Levantine Basin (as discussed earlier.) During the winter period, the overall picture of the Aegean Sea is more uniform in terms of both absolute values (36–39 psu) and the spatial distribution of SSS. In contrast, the highest salinity differences and most pronounced zonation occur in summer.

Satellite data have been used to provide a quantitative impression of the interannual monthly variability in the thermal structure of the surface waters of the Aegean Sea. Straightforward correlation with SST is not possible due to the lack of corresponding in-situ observations. The satellite data used consists of sectorised enlargements of AVHRR (Advanced Very High Resolution Radiometer) grey-tone thermal images from NOAA-9 and NOAA-11 satellites,

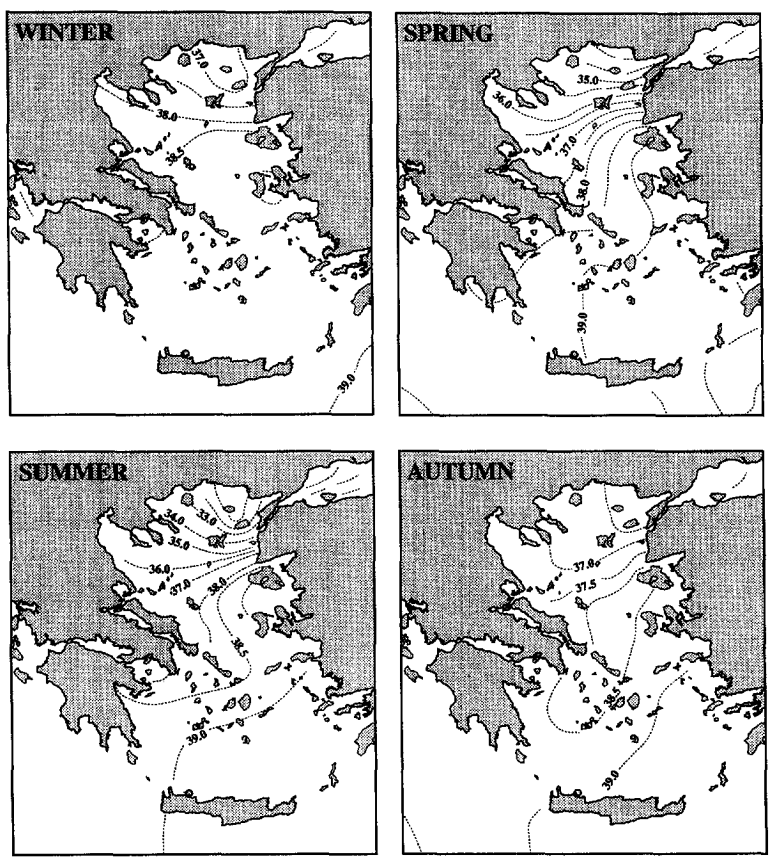

Fig. 11. Seasonal spatial distribution in sea surface salinity (in psu) over the Aegean Sea.

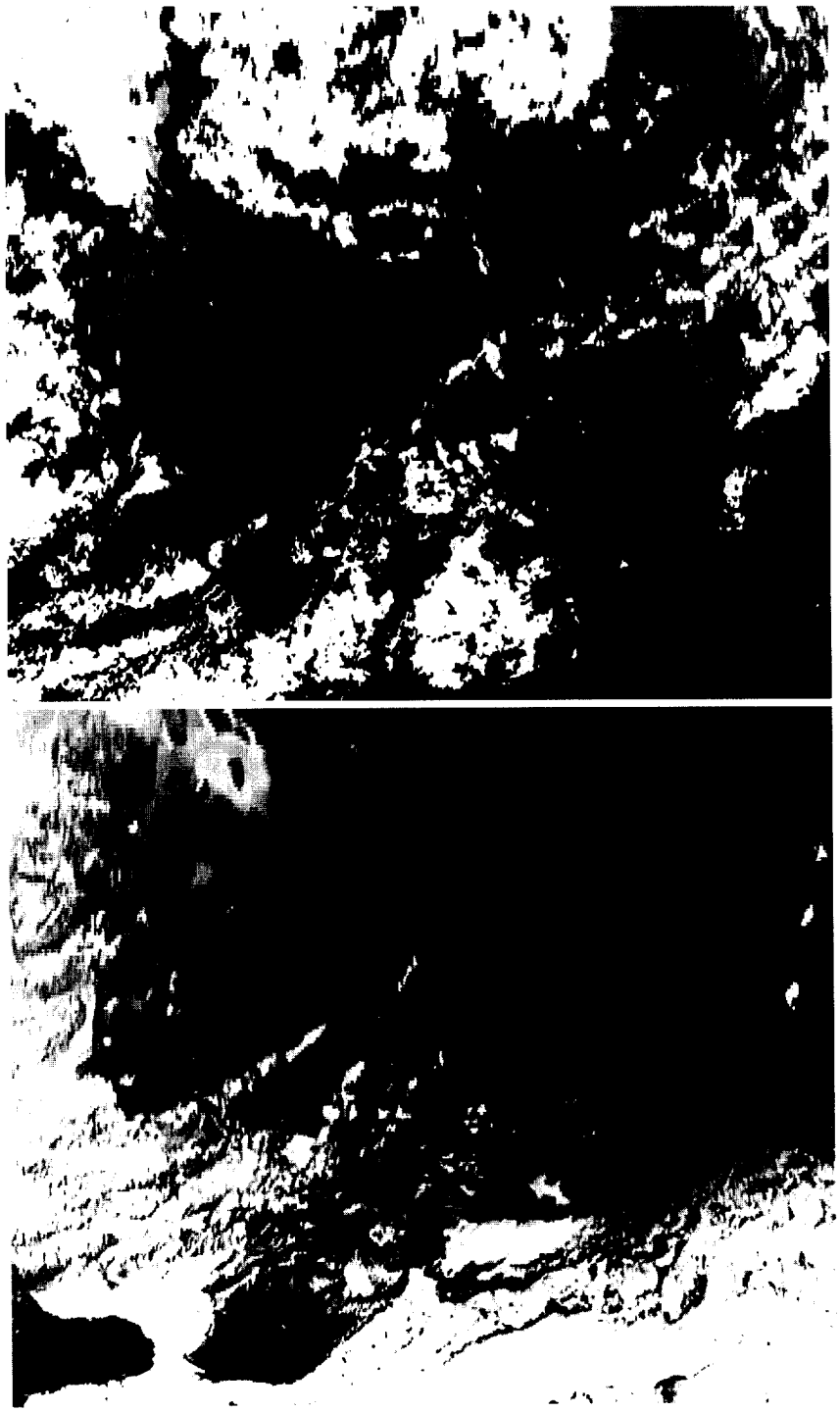

Plate 1. AVHRR image of the Aegean Sea obtained on 19th, January 1993 (Note: The lighter shade indicates the presence of colder surface waters).

Plate 2. AVHRR image of the Aegean Sea obtained on 6th, May 1989 (Note: The lighter shade indicates the presence of colder surface waters).

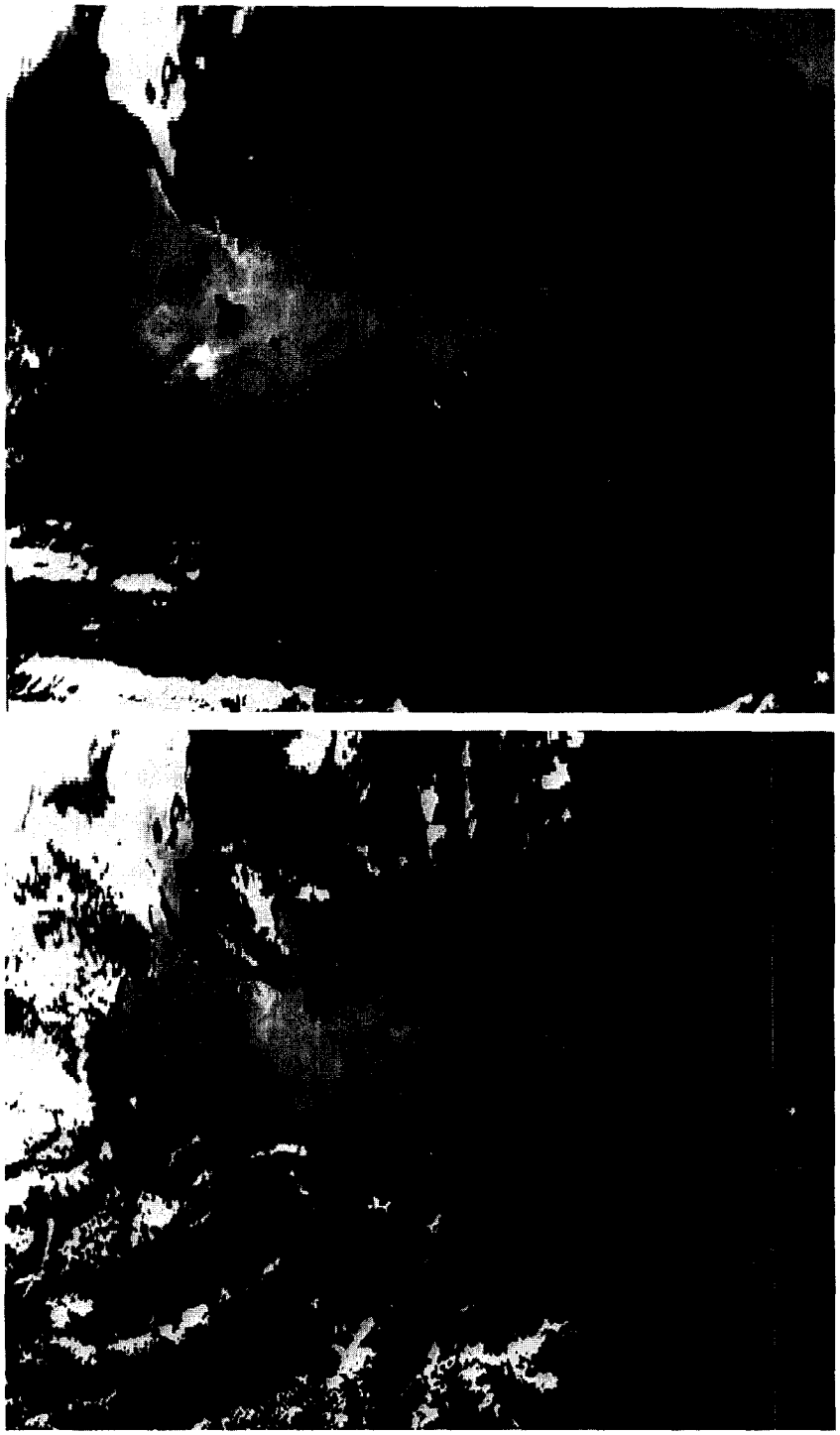

Plate 3. AVHRR image of the Aegean Sea obtained on 11th, August 1989 (Note: The lighter shade indicates the presence of colder surface waters).

Plate 4. AVHRR image of the Aegean Sea obtained on 13th, October 1990 (Note: The lighter shade indicates the presence of colder surface waters).

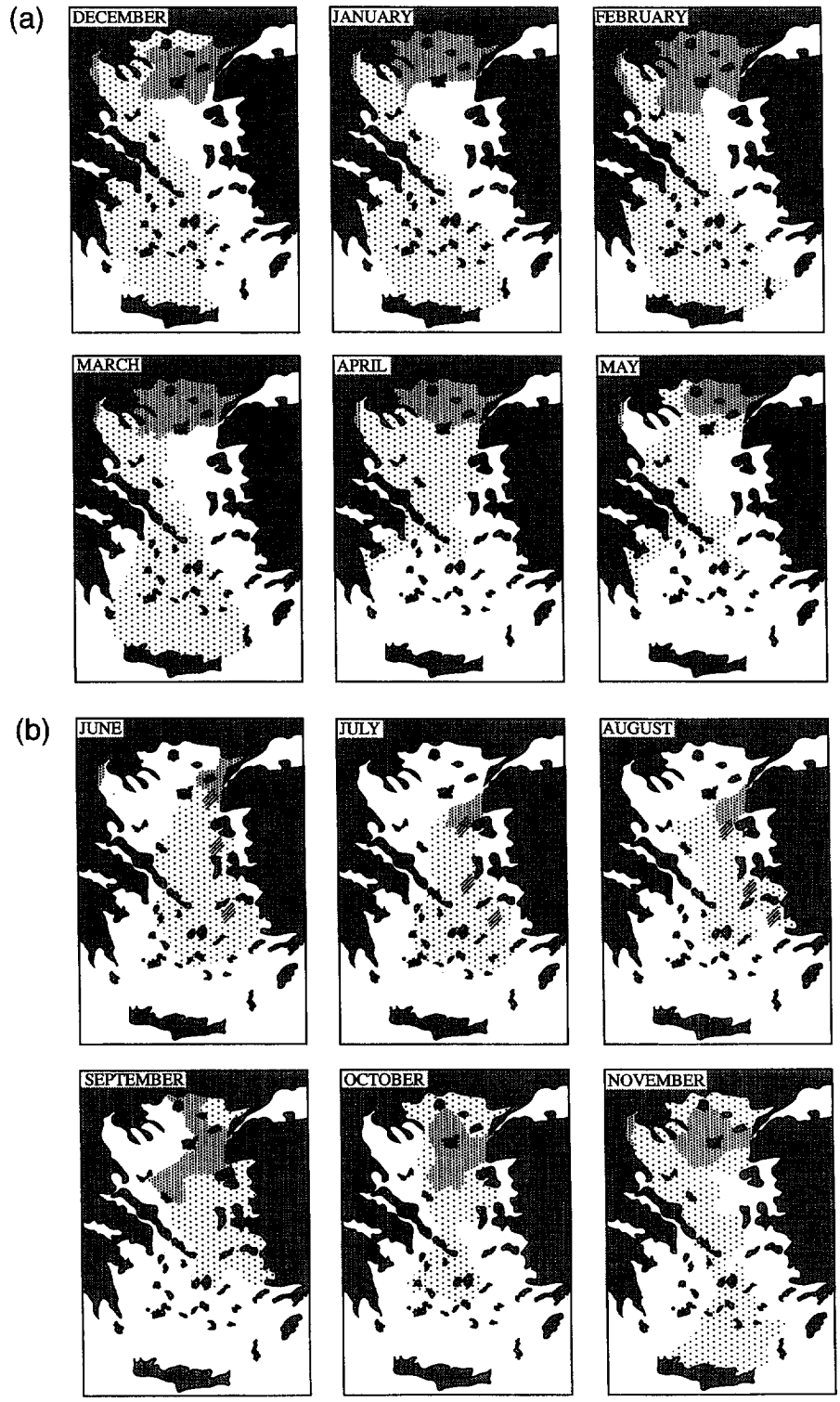
(a)
DECEMBER
JANUARY
FEBRUARY
MARCH
APRIL
MAY
(b)
JUNE
JULY
AUGUST
SEPTEMBER
OCTOBER
NOVEMBER

within the 10.5–12.5 μ wavelength range. These data cover the period June 1988 to May 1994 and consist of a series (116) of images with cloud cover < 10%. The remotely-sensed satellite data available are somewhat restricted, as the Aegean Sea is located near or outside the NOAA acquisition range at Lannion (France). In Fig. 12 the monthly variability in the distribution of the relatively colder water masses (i.e. BSW, upwelling phenomena) are presented schematically, whilst actual representative images for each season are presented in Plates 1–4.

In general, the SST distributional patterns in winter and summer can be identified as the principal ones (see below); spring and autumn can be characterised as transitional periods.

7.1. Winter (January–March)

In winter, there is a zonal distribution of SST with values increasing towards the southeast (Fig. 10). The colder waters (< 14°C) dominate the northern part of the Aegean Sea, as a result of the relatively colder and less saline BSW inflow and that at the main river systems discharging into the area (see Fig. 1). The relatively warmer waters (> 16°C) occupy the eastern part of the Cretan Sea and adjacent straits, being attributed to the Levantine inflow.

Furthermore, the main body of the cold water mass (mostly BSW, with secondary river inputs) extends towards the west, as far as the western extremity of the Kassandra Peninsula (in January and February), reaching the Sporades Islands towards the southwest (Fig. 12). There would appear to be little or no penetration of these surface waters into the Gulfs of Chalkidiki. Besides, the cold waters present along the northern Aegean coastline and within Thermaikos Gulf may be attributed also to colder freshwater river inputs. In particular, the Thermaikos river inputs are transported along the western coastline of the Aegean Sea, forced occasionally by the locally northerly (Vardar) wind, funneled along the valley of the R. Axios (Robles et al., 1983).

The relatively colder waters (BSW and river inputs) move in a southerly direction along the western coast of the Greek mainland; they reach the eastern Peloponesos and occupy, in general, the western part of the Aegean Sea (Fig. 10).

Fronts appear at the boundary between the cold waters in the northern and northwestern parts of the Aegean Sea and the warmer waters of the southeastern part. A similarly strong thermohaline front has been identified over the Limnos Plateau, where the colder and less saline BSW encounters the warmer and more saline Levantine Waters (LW) (Theocharis and Georgopoulos, 1993). Such fronts can be identified in Plate 1. Moreover, the LWs tend to intrude intermittently towards the Samothraki Plateau, producing remarkable temporal and spatial variability.

7.2. Spring (April–June)

In spring (mainly April and May), as a result of cooling and wind mixing which has occurred during winter, SST isopleths present a more complex picture (Fig. 10) with values varying, in general, between 18.5 and 19.5°C; this corresponds to a maximum gradient of 0.2–0.3°C km^{-1}. During May, there is essentially minimal frontal expression in the eastern Mediterranean Sea (Phillipe and Harang, 1982). However, numerous eddies and wave-like features appear on the corresponding satellite image of the Aegean Sea (Plate 2).

Monthly satellite imagies indicate that, during spring, the main cold water mass is restricted to the northeastern Aegean Sea (Fig. 12). A relatively colder water mass diffuses widely and initially into the northern and eastern part and, subsequently, to the central part of the Aegean Sea; it extends then farther to the south, over the Cyclades Plateau. The cold water masses within Thermaikos Gulf are attributed to the high discharge levels of the rivers Axios, Aliakmon, Pinios (cf. Fig. 7).

7.3. Summer (July–September)

In summer, SST varies from 22°C, at the entrance to the Dardanelles and within inner Thermaikos Gulf, to more than 24°C within the Cretan Straits. There is

Fig. 12. Generalised interpretation showing the monthly thermal distribution over the Aegean Sea, based upon the interpretation of satellite imagery. Note: denser shading indicates colder water.

a general increase in SST of 2–3°C, from east to west. The lower values along the eastern coastline and, partially in the central Aegean Sea, may be attributed to an upwelling phenomenon induced by the Etesians [the prevailing wind condition which blow generally from N-NE directions (cf. Fig. 2)]. Fig. 12 and Plate 3 show that a relatively colder zone occupies the central and southeastern part of the Aegean Sea, associated with upwelling phenomena. The cooling of the sea surface causes also high static atmospheric stability and, hence, stable weather conditions which render the channeling effect of the Etesians much more effective (Metaxas, 1973).

The Etesian winds also cause downwelling along the eastern coastline of Greece; this strengthens the existing southerly longshore flow along the western part of the Aegean Sea (Lascaratos, 1992). Besides, during summer (July–August), the river discharges are minimal and contribute only indirectly to the maintenance of relatively warmer waters over the northern and western parts of the Aegean Sea.

7.4. Autumn (October–December)

The autumn can be characterised as a transitional period with: (i) gradual cessation of the Etesians (at the end of September); (ii) the river discharges increasing gradually (after October) and (iii) the BSW reestablishing itself as the dominant hydrological feature. At the same time, warm water intrusions from the Levantine Basin take the place of summer upwelling over the eastern part of the area. Temperatures of the surface waters range from 15–20°C, with the SST isopleths presenting a rather complex picture denoting the transition from the summer to the winter distributional pattern (Fig. 10).

During autumn (Fig. 12), the relatively colder waters are restricted to the northern parts of the Sea (in October and November), whilst the BSW spreads gradually over the northeastern part of the Aegean Sea. In addition, the cold riverine waters spread out over the region i.e. within Thermaikos Gulf.

Interesting composite features present in the image for this period (Plate 4) are the tongues of BSW extending northwards, up to the island of Thasos. An analogous situation has been identified, on the basis of the analysis of in-situ SST data, by Roufogalis (1971b).

8. Summary

The Aegean Sea is the northeastern extension of the Mediterranean Sea; it experiences, therefore, a "Mediterranean-type" of climate with mean monthly air temperatures varying between 5°C (in winter) and 27°C (in summer). Precipitation is, in general, between 350 and 700 mm yr^{-1}; for comparison, the mean annual evaporation is of the order of 3.5–5 mm d^{-1}. The prevailing climatological conditions fluctuate seasonally, with higher air temperatures occurring during the warmer and drier period (May–September).

The region is characterised by a negative heat budget ($Q_s < Q_b + Q_e + Q_h$), of the order of -26 Wm^{-2}. This deficit implies the loss of heat through the surface, with the balance maintained by the advection of water masses.

The Aegean Sea receives freshwater inputs from rivers and ephemeral streams discharging along its coastline; these amount to approximately 2×10^{10} m^3 yr^{-1}. Further, it receives some 3×10^{11} m^3 per annum of relatively colder and less saline Black Sea Waters, through the Darardanelles Strait. The overall water balance of the Aegean basin, without taking into account the exchange of water masses through the Cretan Straits, is positive 1.0–1.4 m yr^{-1}. This water mass surplus, despite the high rate of evaporation, may be attributed to the Black Sea Water inflow to the Aegean Sea.

Water circulation within the Aegean Sea is controlled by the prevailing wind conditions and the thermohaline circulation patterns and their seasonal variability. Winds blow mainly from the north, whilst some south-southwesterly winds blow during spring. Moderate diurnal sea-breezes are also present along the coastline. During summer, the (northerly) Etesians dominate the wind field over the Sea, reaching gale force speeds. A spatially and seasonally consistent water circulation pattern for the whole of the Aegean Sea is very complex, due to the high variability of the wind regime and the complex geomorphological configuration of the Aegean Sea basin. The surface water circulation is incorporated, in general, into an anti-clockwise gyre system during winter. In summer, water movement is essentially towards the south.

Sea surface temperatures (SST) and salinities

(SSS) fluctuate spatially and seasonally. Mean monthly SSTs vary from 8°C in the north during winter, up to 26°C in the south during summer. SSS values vary from less than 31.0 psu, in the north, up to more than 39.0 psu, in the southeast, presenting their maximum differences during summer; during winter and autumn, the distribution of SSS values is more uniform. The overall seasonal spatial distribution pattern of SST and SSS values is dependent upon: (a) the distribution of the colder Black Sea Waters; (b) the advection of the warmer Levantine Waters, from the southeast; (c) upwelling induced by the Etesians; and (d) to a lesser extent but locally important, freshwater riverine outflows.

Acknowledgements

The authors are grateful to Prof. H. Charnock for his constructive comments and guidance. We would like to acknowledge the Hellenic Meteorological and Hydrographic Services, who kindly provided part of the data set. Thanks are extended also to the NERC Satellite Receiving Station, University of Dundee, for making available a series of AVHRR satellite images. Mrs. K. Davis is acknowledged for her artistic representation of the Figures. Finally, during the preparation of the manuscript one of the authors (SP) was supported by the EU "Human Capital and Mobility" programme (Contract No. 941769).

References

Bethoux, J.-P., 1980. Mean water fluxes across sections in the Mediterranean Sea, evaluated on the basis of water and salt budgets and of observed salinities. Oceanol. Acta, 3(1): 79–88.

Bethoux, J.P. and Gentili, B., 1994. The Mediterranean Sea, a test area for marine and climatic interactions. In: P. Malanotte-Rizzoli and A.R. Robinson (Editors), Ocean Processes in Climate Dynamics: Global and Mediterranean Examples. Nato ASI Ser., C: Math. Phys. Sci., 419. Kluwer, Dordrecht, pp. 239–254.

Bignami, F., Santoleri, R., Schiano, M. and Marullo, S., 1991. Net longwave radiation in the Western Mediterranean Sea. Poster Session 20th General Assembly Int. Union Geodesy Geophys., IAPSO, Vienna, August 1991.

Blumberg, A.F. and Mellor, G.L., 1987. A description of a three-dimentional coastal oean circulation model. In: N.S. Heaps (Editor), Three-Dimensional Coastal Ocean Circulation Models. Coastal Estuarine Sci., 4, AGU, Washington, D.C., pp. 1–16.

Brasseur, P., Beckers, J.M., Brankart, J.M. and Schoenauen, R., 1996. Seasonal temperature and salinity fields in the Mediterranean Sea: Climatological analyses of an historical data set. Deep-Sea Res., 43: 159–192.

Bunker, A.F., 1971. Wintertime interactions of the atmosphere with the Mediterranean Sea. J. Phys. Oceanogr., 2: 225–238.

Bunker, A.F., Charnock, H. and Goldsmith, R.A., 1982. A note on the heat balance of the Mediterranean and Red Seas. J. Mar. Res., 40(suppl.): 73–84.

Businger, J.A., Wyngaard, J.C., Izumi, Y. and Bradley, E.F., 1971. Flux profile relationships in the Atmospheric Surface Layer. J. Atmos. Sci., 28: 181–189.

Carapiperis, L.N., 1968. The Etesian Winds. Mem. Natl. Obs. Athens, Ser. II. Meteorology, 17, 19 pp.

Catsoulis, V.D., 1970. The Wind Conditions in the Aegean Sea. Ph.D. Thesis, Univ. Athens (in Greek). (unpubl.)

Ergin, M., Bodour, M.N. and Ediger, V., 1991. Distribution of surficial shelf sediments in the northeastern and southwestern parts of the Sea of Marmara: Strait and canyon regimes of the Dardanelles and Bosporous. Mar. Geol., 96: 313–340.

Garrett, C., Outerbridge, R. and Thomson, K., 1993. Interannual variability in Mediterranean heat and buoyancy fluxes. J. Climatol., 6: 900–910.

Gilman, G. and Garrett, C., 1994. Heat flux parameterizations for the Mediterranean Sea: The role of atmospheric aerosols and constraints from the water budget. J. Geophys. Res., 99: 5119–5134.

Hopkins, T.S., 1978. Physical processes in the Mediterranean Basins. In: B. Kjerfve (Editor), Estuarine Transport Processes. Univ. South Carolina Press, Columbia, pp. 269–306.

Jakovides, C., Papaioannou, G. and Michalopoulou, H., 1989. Evaporation over the Aegean Sea using large-scale Parameters. Meteorol. Atmos. Phys., 41: 255–260.

Kaufeld, L., 1981. The development of a new Beaufort equivalent scale. Meteorol. Rundsch., 34: 17–23.

Lacombe, H. and Tchernia, P., 1972. Caracteres hydrologiques et circulation des eaux en Mediterranee. In: D.J. Stanley (Editor), The Mediterranean Sea. Dowden, Hutchinson and Ross, Stroudsberg, pp. 26–36.

Lascaratos, A., 1992. Hydrology of the Aegean Sea. In: H. Charnock (Editor), Winds and Currents of the Mediterranean Basin. Rep. Meteorol. Oceanogr., 40. Harvard Univ., Cambridge, 1, pp. 313–334.

May, P.W., 1982. Climatological Flux Estimates in the Mediterranean Sea: Part I. Winds and Wind Stresses. Naval Ocean Research and Development Activity, Rep. 54, NSTL Station, Mississippi 39529, 53 pp.

May, P.W., 1983. Climatological Flux Estimates in the Mediterranean Sea, vol. 2. Air Sea Fluxes. NORDA Rep., 58, Nav. Ocean Res. Dev. Activ., NSTL Station, Miss., 65 pp.

Metaxas, D.A., 1973. Air–sea Interaction in the Greek Seas and Resulted Etesian Wind Characteristics. Univ. Ioannina, Tech. Rep., 5, 32 pp.

Nittis, K., Lascaratos, A. and Perivoliotis, L., 1995. A Numerical Study of the Aegean Sea General Circulation. Rapp. Comm.

Int. Mer Medit., XXXIVe Congres de la CIESM, La Valette, Malte, vol. 34, 190 pp.

Oguz, T. and Sur, I.H., 1989. A two-layer model of water exchange through the Dardanelles Strait. Ocanol. Acta, 12(1): 23–31.

Ovchinnikov, I.M., 1966. Circulation in the surface and intermediate layers of the Mediterranean. Oceanology, 6: 48–59.

Phillipe, M. and Harang, L., 1982. Surface structure fronts in the Mediterranean Sea from infrared satellite imagery. In: J.C.J. Nihoul (Editor), Hydrodynamics of Semi-enclosed Seas. Elsevier, Amsterdam, pp. 91–128.

Reed, R.K., 1977. On estimating insolations over the ocean. J. Phys. Oceangr., 17: 854–871.

Robles, F.L.E., Collins, M.B. and Ferentinos, G., 1983. Water masses in Thermaikos Gulf, north-western Aegean Sea. Estuarine Coastal Shelf Sci., 16: 363–378.

Roether, W., Manca, B., Klein, B., Bregant, D., Georgopoulos, D., Beitzel, V., Kovacevic, V. and Luchetta, A., 1996. Recent changes in eastern Mediterranean deep waters. Science, 271: 333–335.

Rougogalis, V., 1971a. Oceanographic study of the North Aegean Sea. Hellenic Hydrogr. Serv. Publ., 1 (in Greek).

Roufogalis, V., 1971b. Oceanographic observations in the South Aegean Sea. Hellenic Hydrogr. Serv. Publ., 2 (in Greek).

Smith, S.D., 1988. Coefficients for sea surface wind stress, heat flux, and wind profils as a function of wind speed and temperature. J. Geophys. Res., 93: 15,467–15,472.

Theocharis, A., Georgopoulos, D., Karagevrekis, P., Iona, A., Perivoliotis, L. and Charalambidis, N., 1992. Aegean influence int he deep layers of the eastern Ionian Sea (October 1991). Rapp. Comm. Int. Mer Medit., 33: 235.

Theocharis, A. and Georgopoulos, D., 1993. Dense water formation over the Samothraki and Limnos Plateaux in the north Aegean Sea (Eastern Mediterranean Sea). Continental Shelf Res., 13(8/9): 919–939.

Theocharis, A., Georgopoulos, D., Lascaratos, A. and Nittis, K., 1993. Water masses and circulation in the central region of the Eastern Mediterranean: Eastern Ionian, South Aegean and Northwest Levantine, 1986–1987. Deep-Sea Res., II 40(6): 1121–1142.

Theodorou, A.J., 1992. Physical oceanographic studies for the design of the Athens Sea outfall (Saronikos Gulf, Greece). Water Sci. Technol., 25(9): 31–40.

Theoharatos, G.A. and Tselepidaki, I.G., 1990. The temperature of the sea-surface in the region of the Aegean and its relation to air temperature. Theor. Appl. Climatol., 42: 117–119.

Therianos, A.D., 1974. Rainfall and geographical distribution of river runoff in Greece. Bull. Geol. Soc. Greece, XI: 28–58 (in Greek).

Tixeront, J., 1970. Le bilan hydrologique de la mer noire et de la Mer Mediterranee. Cah. Oceanogr., 22: 227–237.

Tolmazin, D., 1985. Changing coastal oceanography of the Black Sea. II: Mediterranean effluent. Prog. Oceanogr., 15: 277–316.

Unluata, U., Oguz, T., Latif, M.A. and Ozsoy, E., 1990. On the physical oceanography of the Turkish Straits. In: L.J. Pratt (Editor), The Physical Oceanography of Sea Straits. Kluwer, Dordrecht, pp. 25–60.

Vlahakis, G.N. and Pollatou, R.S., 1993. Temporal variability and spatial distribution of sea surface temperatures in the Aegean Sea. Theor. Appl. Climatol., 47: 15–23.

Woodruff, S.D., Sleutz, R.J., Jenne, R.L. and Steurer, P.M., 1987. A comprehensive ocean–atmosphere data set. Bull. Am. Meteorol. Soc., 68: 1239–1250.

Yuce, H., 1996. On the variability of mediterranean water flow into Black Sea. Continental Shelf Res., 16: 1399–1413.

Zabakas, J.D., 1981. General Climatology. Univ. Athens Press, 493 pp. (in Greek).

Zodiatis, G., 1993. Circulation of the Cretan sea water masses (Easten Mediterranean). Oceanol. Acta, 16(2): 107–114.

Zodiatis, G. and Balopoulos, E., 1993. Structue and characteristics of fronts in the north Aegean Sea. Boll. Oceanol. Teor. Appl., XI(2): 113–124.

Zodiatis, G., 1994. Advection of the Black Sea water in the north Aegean Sea. Global Atmos. Ocean Syst., 2(1): 41–60.